Influence of the electrochemical treatment on the magnetic properties of nanowires

George Tepes*, Alecs Andrei Matei, Maria Diana Vranceanu, Cosmin Mihai Cotrut, Dionezie Bojin

University POLITEHNICA of Bucharest, Faculty of Materials Science and Engineering, Bucharest, **060042, Romania.**

Victor Kuncser

National Institute for Physics of Materials, Magurele, P.O. Box MG 7, Bucharest, 77125**, Romania**

Ruxandra Vidu

University of California, Davis, Department of Chemical Engineering and Materials Science, Davis CA 95616, United States of America
Corresponding Author: *tepes.george@gmail.com

Abstract: Synthesis of nanomaterials is one of the most researched areas. Nanomaterials are at the core of all modern nano-devices. The reduced size helps electronics to have increased performance, low energy consumption and low heat output. Properties of nanomaterials are mainly related to the involved large surface to volume ratio. Nanomaterials can be fabricated using different methods. One of the intensely used, inexpensive and with high degree of reproducibility is electrochemistry (EC), which can be used either to destroy (corrosion) or to create (thin films, nanoparticles, nanowires (NWs), etc.) materials. In this paper we focus on the effect of the electrochemical treatment (EchT) on the structural and magnetic properties of nanowires. Ni NWs were synthesized and analyzed by SQUID to study the magnetic properties induced by the EchT of the Au substrate. Ni NWs were synthesized in a gold-coated PCTE membrane using template synthesis. The EchT induced structural modifications of the Au substrate and further modifications of NWs magnetism.

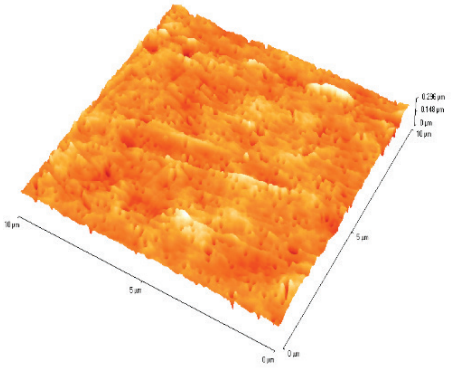

AFM image of the Au plated PCTE template

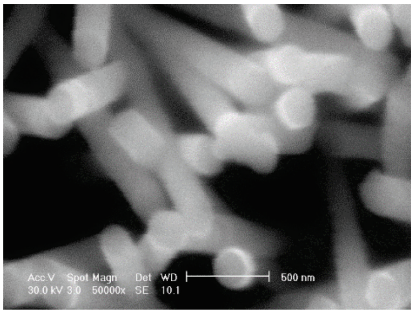

SEM image of Ni Nanowires

1. Introduction

Common materials such as Fe, Co, Ni exhibit special chemical and physical properties when they have two dimensions in the nanometer range (i.e. nanotubes, nanowires or nanocables). This could be the main reason why after decades of researches all over the world there is still interest in studying properties of common 1-dimmensional nanomaterials [1-4]. This particularity makes materials to exhibit interesting behavior compared to bulk materials, which can be exploited in order to create more energy efficient materials, with improved magnetic properties at room temperature (i.e. giant magnetic resonance, giant magnetostriction [2, 5]) and enhanced mechanical resistance.

Ni is one of the metals that shows property changes when two dimensions are in the nanometer scale with the third much larger [6]. Nickel can be used in many applications, including biomedicine, sensors (general or biological), electrical devices, transparent conducting circuits [7], printable electronics, etc. For all these applications, the nanowire is the most investigated shape [8-11].

Nanowires (NWs) are commonly synthesized with high reproducibility using template based electrodeposition (ED) [3, 12-14]. Template synthesis consists in the electrodeposition of an electrically conductive element from an aqueous solution inside the transversal pores of a membrane. Before the nanowire growing process, the membrane is sputter coated on one side with a thin conducting film.

After the application of a conducting layer on the template, the sample is sandwiched in between two insulated tapes, leaving a small opening for the working electrode (WE) surface (Figure 1). Then, the sample is immersed together with a reference electrode (RE) and a counter electrode (CE) in an aqueous solution in a 3-electrode cell configuration (Figure 2). This paper presents another step that was implemented to increase the experimental reproducibility. This step consists of an electrochemical treatment of the conducting layer that coat the template surface, e.g. an Au thin film in the present case. It has been reported that during the electrochemical treatment applied to Au surface, a high surface diffusion process develops leading to a smoother electrode surface [15-21]. This electrochemical treatment, similar with a thermal annealing process, is performed at room temperature in 50 mM H_2SO_4 [22-24].

Superconducting Quantum Interference Device (SQUID) technique (MPMS XL from Quantum Design, USA) was used to measure the magnetic properties of the NWs grown in PCTE template. The SQUID device has a high sensitivity and reproducibility (i.e. 10^{-8} emu resolution in magnetic moment, maximum field of 7T, 10^{-4}T field resolution, and temperature range from 2K to 400K with 10^{-3} K stability).

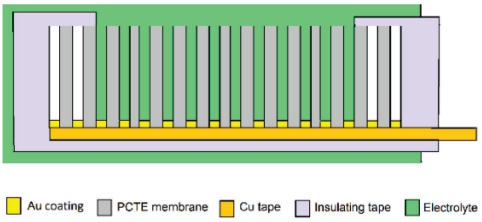

Figure 1. Setup configuration for NWs ED sample

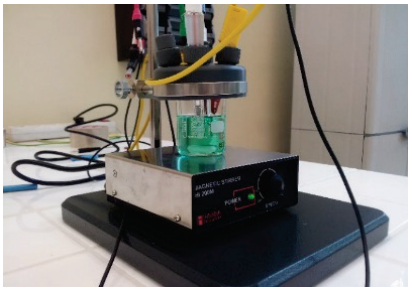

Figure 2 The 3-electrode electrochemical cell

X-ray diffraction (XRD) measurements were performed using an APD 2000 diffractometer (GNR, Agrate Conturbia Novara, Italy) in Bragg-Brentano

configuration, The experiments were performed at 2θ with a range from 37° to 82°, a step of 0.02° and a measuring time of 1 s for each step, using the Cu Kα radiation (λ = 1.54 Å), X-ray tube high voltage of 40 kV and tube current 30 mA.

2. Experimental

2.1. Sample preparation

Commercially available polycarbonate track-etched membranes (PCTE, GE OSMONICS INC, USA) with a thickness of 6 µm, a density of $4x10^9$ pores/cm^2 and pore diameter of 100 nm, (as quoted by supplier) were used as template. Nickel (II) sulphate hexahydrate ($NiSO_4 \cdot 6H_2O$), boric acid (H_3BO_3) and dichloromethane (CH_2Cl_2) were purchased from Sigma-Aldrich, Germany. The electrolytes were freshly prepared from high purity chemical compounds and ultrapure water (ASTM I, 18 MΩ.cm).

Electrochemical deposition of Ni NWs was performed using a PARSTAT 4000 Potentiostat/Galvanostat (Princeton Applied Research - AMETEK) equipped with a three electrodes cell setup. A custom working electrode (WE) made from two isolating tapes, cupper tape and PCTE template with pore diameter of 100nm, coated with Au on one side (Figure 1) were used. A saturated calomel electrode (SCE) was the reference electrode and a platinum rod was the counter electrode (CE). All reported potentials are with respect to the reference electrode. The electrolyte had the following chemical composition: 44 gl^{-1} $NiSO_4 \cdot 6H_2O$, 40 gl^{-1} H_3BO_3 and ultrapure water (ASTM I, 18 MΩ·cm) for Ni NWs growth and 50 mM H_2SO_4 for electrochemical treatment of Au layer.

2.2. Sample characterization

After sputtering the gold on the PCTE membrane, the working electrode is produced according to the design presented in Figure 1. Then, the sample is cleaned up and treated to assure reproducible results. Cleaning is the first step of the electro-chemical treatment and consists of 12 voltammetry cycles at a sweep rate of 50 mV/s in 50 mM H_2SO_4. The second step consists of maintaining the potential for 10-15 minutes at a value before the peak oxidation of Au to allow surface diffusion. Figure 3 presents the cyclic voltammograms before and after the electro-chemical treatment of the WE. The difference in the electrochemical behavior clearly indicates that the applied electrochemical treatment (EchT) induces major changes on the Au surface. The EchT allows atoms to rearrange on the surface. Surface diffusion of Au atoms was studied by Hirai et al. [24] using an electrochemical atomic force microscopy (EC-AFM). They reported the filling of the empty sites in the low-level terraces with atoms that decay from the top atomic terraces. Comparable results have are reported at room temperature on the potential-dependent morphologies [22-26].

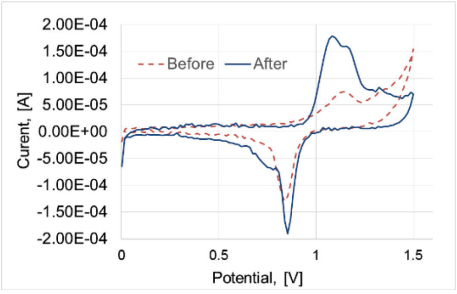

Figure 3. Cyclic voltammetry of Au film in 50mM H_2SO_4 before and after EchT (v = 50mV/s)

During the surface diffusion process at ~0.9 V, there are no oxidation/reduction reactions. At this potential, the surface accumulates an excess of positive charge. In consequence, a repulsive force between atoms appears and forces them to have high mobility. This mobility is amplified by the electric double layer that can attract atoms which are at the interface between surface and electrolyte. It results a more uniform crystalline structure and a

smoother surface. Recent reports have shown that a gold substrate can influence the crystal development of the NWs/films grown on it [27].

To investigate this effect on Ni NWs, 2 types of samples (Au films) were prepared. The EchT consisted of 12 CV followed by maintaining the potential constant at 0.85V for different periods of time in 50 mM H_2SO_4. The only difference between samples was the duration of applied potential, i.e. 60 and 120 minutes.

On each sample a detailed XRD analysis was performed to measure and calculate the lattice parameter, crystallite size, and the texture coefficient. For all the investigated specimens we performed 3 measurements using same conditions for a better accuracy of the results. The crystalline phase compositions of the investigated specimens were established based on ICDD data files (Figure 4).

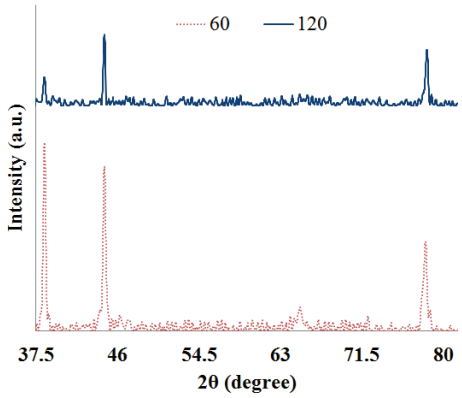

Figure 4. XRD spectra of Au at different EchT times; EchT was performed through the pores

All the XRD peaks were indexed by face-centered cubic gold phase (ICDD gold card No. 04-0784). The calculated inter-planar distance (d) are in accordance with the inter-planar distance (d) from ICDD gold card. In the Au face-centered cubic structure, the d is related to the lattice constant (a) and the Miller indices by the following equation [28]:

$$d_{hkl} = \frac{a}{\sqrt{h^2+k^2+l^2}} \qquad (1)$$

The calculated *a* for all investigated specimens are given in Table 1. The *a* values are compared with *a* value form ICDD data card using corresponding (hkl) planes and the percentage of variation of *a* is below 1%. Because the differences among inter-planar distances of investigated samples and ICDD data card are less than 1%, the stress in specimens is quite small.

	2θ	FWHM	I/I0	hkl
60	38.4	0.292	100	111
	44.66	0.341	72	200
	78.2	0.612	32	311
120	38.46	0.407	25	111
	44.66	0.226	50	200
	78.26	0.331	100	311
	d (A)	**a**	**D (nm)**	**TC (hkl)**
60	2.3434	4.05893	31	0.9
	2.0284	4.05679	28	1.3
	1.2219	4.05261	19	0.8
120	2.3399	4.05284	23	0.2
	2.0284	4.05679	42	0.7
	1.2211	4.05	34	2.1

Table1. Calculated parameters from XRD patterns

The peak broadening in the XRD pattern clearly indicates that small crystallites are present in the specimens. Thus, we calculate the average crystalline size (D) using the Scherrer equation (Eq. 2):

$$D = \frac{k\lambda}{\beta\cos(\theta)} \qquad (2)$$

where k is the Scherrer constant and its equal to 0.9, λ is the wavelength of the radiation, β is the integral width expressed in radians, θ is the Bragg angle of the peak. The average crystallite size for different (hkl) Miller indices, are given in Table 1. The average crystallite size is about 33 nm for the samples treated for 120 minutes, while for the specimen treated for 60 min the average crystallites size is 26 nm.

Using the "texture coefficient" TC (hkl), we have estimated the texture of the specimens. TC can be expressed as:

$$TC(hkl) = \frac{I(hkl)/I_0(hkl)}{1/n\sum_n I(hkl)/i_0(hkl)} \quad (3)$$

where I(hkl) is the measured relative intensity of the (hkl) peak, I_0(hkl) is the standard intensity assigned to the same (hkl) planes and n is the number of peaks used to assess the TC. When TC (hkl) > 1 an abundance of crystallites oriented with <hkl> direction is indicated. The XRD patterns (Fig.4) clearly show that the treated sample at 120 minutes have preferential orientation. The (311) lines of gold treated at 120 minutes are about two times more intense than (111) ones which show that <311> is the preferred growth direction. Surprisingly, the specimen treated for 60 min indicate no preferential orientation of the gold crystallites.

After the XRD analysis on samples Ni NWs were electrochemical deposited on the Au substrate through the PCTE pores. To ensure a good homogeneity the electrolyte was stirred with a magnetic stirrer. Deposition was carried out in pulse with a frequency of 10 pulses/s between 0 and -1 V for 20 minutes deposition time.

After the synthesis of Ni NWs the samples were prepared for magnetic characterization. Each sample (array of NWs) was cut in a small rectangular shape with an area of ~0.9 mm^2. The magnetic field was applied either parallel or perpendicular to the sample plane. Hysteresis loops taken at 10 K with parallel field are presented in Figure 6. Accordingly, there are clear differences between the two samples (i.e. same EC growth conditions for Ni NWs).

These differences could be induced by the quantity of Ni NWs or by the crystallite sizes. To establish the main effects on the magnetic properties, the amount of Ni in each sample was estimated. First, the number of pores on each sample was calculated based on the sample surface area (i.e. ~ 9 mm^2), the estimated numbers of pores (400 pores/100um^2) and the estimated filling of pores. Calculations were performed by averaging 10 area measurements and taking into account that at a given electrodeposition time, approx. 40% of pore length is filled. The results are presented in Table 2. According to the above results, a specific magnetization of about 65(9) emu/g is obtained for sample 60 and 67(9) emu/g for sample 120.

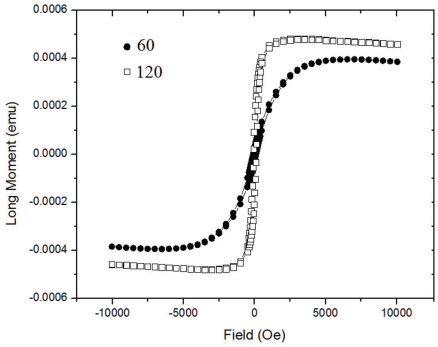

Figure 6. Magnetic hysteresis loops at 10 K (parallel field) for the samples

Sample	60	120
Area, mm^2	10(1)	11(1)
Nr of pores	37(3)E6	43(3)E6
Ni, g	6(1)E-06	7(1)E-06

Table 2. Quantity of Ni in each sample

This results correspond in the error limits to the specific magnetization of Ni (58.6 emu/g). Hence, no difference can be attributed to the spontaneous magnetization between the samples. However, the two samples behave differently concerning both the coercive fields and the saturation field which are larger in sample 60. Since the Ni NWs nucleation and growth are dictated by Au substrate, any changes induced by the EchT on Au would affect the nanowire structure as both Ni and Au have same crystalline structure (i.e. face centered cubic crystals). Also, XRD diffractograms demonstrated the modification of Au structure with the applied EchT. This modification could also induce modifications in magnetic properties of

nanowires. Additionally, between the two samples there is a difference of about 20% between crystallite sizes. It is knows that coercivity increases with the crystallite sizes [29, 30].

Conclusions

The nanowire growth was studied to understand the effects of structural changes on the magnetic properties. The structural changes were induced by room-temperature electrochemical treatment, similar to an annealing process, which is usually performed on samples to clean and improve reproducibility. We demonstrated that the duration of the EchT significantly changes the substrate structure and the properties of NWs grown on that surface. A detailed XRD analysis was used to observe any modification that have taken place in the Au crystallographic structure. After synthesis of Ni NWs, a detailed SQUID analysis was performed to quantify any changes that may occur from the magnetic point of view.

From XRD and SQUID resulted that electrochemical treatment induces certain modifications in the Au film. This modification might have been transmitted to the Ni NWs. This research opened the door for more investigations like the magnetic properties of nanostructural materials are interest for many applications.

Acknowledgment

The work has been funded by the Sectorial Operational Program Human Resources Development 2007-2013 of the Ministry of European Funds through the Financial Agreement POSDRU/159/1.5/S/134397. VK acknowledges Core Program PN45103.

References

[1] J. Vilana, E. Gómez, E. Vallés, Journal of Electroanalytical Chemistry 703 (2013) 88-96.
[2] S.S.M. Mahshid, Sara; Dolati, Abolghasem; Ghorbani, Mohammad; Yang, L.; Luo, S.; Cai, Qingyun, Electrochimica Acta 58 (2011) 551-555.
[3] S.L. Cheng, Z.H. Kuo, C.H. Chung, Nanoelectronics Conference (INEC), 2011 IEEE 4th International, 2011, pp. 1-2.
[4] V.L. Mathe, A.D. Sheikh, Physica B: Condensed Matter 405 (2010) 3594-3598.
[5] Z.Z. Sun, J. Schliemann, Physical Review Letters 104 (2010) 037206.
[6] R. Vidu, M. Rahman, M. Mahmoudi, M. Enachescu, T.D. Poteca, I. Opris, Frontiers in systems neuroscience 8 (2014) 91-91.
[7] A.R. Rathmell, Nguyen, M., Chi, M. and Wiley, B. J. , NanoLetters (2012).
[8] Y. Zhang, Y. Liu, L. Su, Z. Zhang, D. Huo, C. Hou, Y. Lei, Sensors and Actuators B: Chemical 191 (2014) 86-93.
[9] B. Weng, S. Liu, N. Zhang, Z.-R. Tang, Y.-J. Xu, Journal of Catalysis 309 (2014) 146-155.
[10] N. Ramgir, N. Datta, M. Kaur, S. Kailasaganapathi, A.K. Debnath, D.K. Aswal, S.K. Gupta, Colloids and Surfaces A: Physicochemical and Engineering Aspects 439 (2013) 101-116.
[11] Z. Liu, W.L. Li, P.P. Jin, W.D. Fei, Journal of Magnetism and Magnetic Materials 345 (2013) 96-99.
[12] B. Jaleh, A. Omidvar Dezfuli, Solid State Communications 166 (2013) 56-59.
[13] J.R. Ku, R. Vidu, R. Talroze, P. Stroeve, JACS 126 (2004) 15022-15023.
[14] D.V. Quach, R. Vidu, J.R. Groza, P. Stroeve, Industrial & Engineering Chemistry Research 49 (2010) 11385-11392.
[15] N. Ikemiya, D. Iwai, K. Yamada, R. Vidu, S. Hara, Surface Science 369 (1996) 199-208.
[16] R. Vidu, S. Hara, Journal of Vacuum Science & Technology B 17 (1999) 2423-2430.
[17] R. Vidu, S. Hara, Scripta Materialia 41 (1999) 617-624.
[18] R. Vidu, N. Hirai, S. Hara, Physical Chemistry Chemical Physics 3 (2001) 3320-3324.
[19] J.R. Ku, R. Vidu, R. Talroze, P. Stroeve, Abstracts of Papers of the American Chemical Society 230 (2005) U2255-U2255.
[20] R. Vidu, J.-R. Ku, P. Stroeve, Journal of Colloid and Interface Science 300 (2006) 404-412.
[21] R. Vidu, S. Li, D.V. Quach, P. Stroeve, Journal of Applied Electrochemistry 42 (2012) 333-339.
[22] N.H. K. Kubo, S. Hara, Applied Surface Science 237 (2004) 301–305.
[23] M.Y. Nobumitsu Hirai, Toshihiro Tanaka, Shigeta Hara, Science and Technology of Advanced Materials 5 (2003) 115–118.
[24] H.T. Nobumitsu Hirai, Shigeta Hara, Applied Surface Science (1998) 506–511.
[25] H.O.a.S.H. Nobumitsu HIRAI, ISIJ International 40 (2000) 702 - 705.
[26] K.-i.W. Nobumitsu Hirai, Akiko Shiraki, and Shigeta Hara, Journal of Vacuum Science & Technology B 18 (2000).
[27] A.M. Thron, P.K. Greene, K. Liu, K.v. Benthem, Acta Materialia 60 (2012) 2668-2678.
[28] B.D. Cullity, Stock, S.R, (2001).
[29] Q. Jin, et al. J. Appl. Phys. 96 (2004) 3452-3457.
[30] A.B. Djurišić, K.H. Tam, Y.F. Hsu, S.L. Zhang, M.H. Xie, W.K. Chan, Thin Solid Films 516 (2007) 238-242.